The glow discharge: an exciting plasma!†

Invited Lecture

JAAS Journal of Analytical Atomic Spectrometry

Annemie Bogaerts

University of Antwerp, Department of Chemistry, Universiteitsplein 1, B-2610 Wilrijk-Antwerp, Belgium

Received 28th January 1999, Accepted 12th April 1999

Glow discharges are used in a large number of application fields. Their use as a spectroscopic source for analytical chemistry is only one application; they are much more widely used for other purposes, such as in the micro-electronics industry and in materials technology, and also as lasers, various kinds of light sources, and in the new upcoming plasma displays. In this review we will give a brief overview of these applications. In order to improve the results in these application fields and, in general, to obtain a better understanding of the plasma processes, various modeling approaches for glow discharges, mainly for the non-analytical applications, have been described in the literature, of which a brief overview will be given here. Finally, our own modeling network, which is specifically applied to analytical glow discharges, will be briefly described and some typical results will be shown.

1 Introduction

The glow discharge is a kind of plasma, which means a partially ionized gas consisting of nearly equal concentrations of positive and negative charges and a large number of neutral species. The glow discharge is formed in a cell filled with a gas (inert or molecular gas) at low pressure. By applying a potential difference between two electrodes, which can either be inserted in a cell or form the cell walls, the glow discharge plasma is created. Indeed, owing to the potential difference, atoms of the discharge gas are ionized to yield free electrons and positively charged ions, which is called 'gas breakdown'. The positive ions are accelerated towards the cathode of the glow discharge, where they can release electrons upon bombardment, called 'secondary electron emission'. The electrons arrive in the plasma, and can give rise to collisions with the gas particles, the most important collisions being excitation and ionization of these gas particles. The excitation collisions, and the subsequent radiative decay to lower levels, result in the characteristic light of the 'glow' discharge (*i.e.*, blue in the case of argon). The ionization collisions create new ions and electrons. The ions can again release electrons from the cathode material; the electrons can, in turn, give rise to new ionization collisions, creating new ion–electron pairs. This electron–ion multiplication process makes the glow discharge a self-sustaining plasma. More information about the operating principles and characteristics of glow discharge plasmas can be found, *e.g.*, in ref. 1–5.

Glow discharges are used in a large number of application fields, ranging from analytical chemistry (which constitutes only a small fraction), to the micro-electronics industry, and also as lasers, light sources, displays, and many other (minor) applications. In this review, we will give a brief overview of these applications, to illustrate that the glow discharge is really an exciting plasma.

Further, to improve the results in the various application fields, a good understanding of the glow discharge processes is desirable. This can be obtained, among others, by mathematical modeling. An overview of the different modeling approaches described in the literature for various kinds of glow discharges will be presented here.

Finally, the insights obtained by the modeling approach make the study of glow discharges very exciting in itself. This will be illustrated by explaining our own modeling network for an analytical glow discharge and the presentation of some typical results.

2 Applications of glow discharges (and related discharges)

As mentioned above, glow discharges are used in a whole range of applications, and not only for analytical chemistry. In order to put the analytical glow discharge in a broader perspective, we will give here an overview of the various (most important) applications.

2.1 Analytical chemistry

The use of the glow discharge for analytical chemistry is based on the principle of 'sputtering'. The material to be analyzed (generally solid samples) is used as the cathode of the glow discharge. The bombardment of positive ions (and other plasma species) at the cathode does not only release secondary electrons, but also atoms of the cathode material, which is called 'sputtering' (*i.e.*, 'sand-blasting' at the atomic level). The atoms of the cathode material arrive in the glow discharge plasma and are subject to collisions with electrons and with other plasma species. The ionization collisions create ions of the cathode material, which can be measured with a mass spectrometer, giving rise to 'glow discharge mass spectrometry' (GDMS) (*e.g.*, ref. 5 and 6). The excitation collisions, and the subsequent radiative decays, emit characteristic photons of the cathode material, which can be detected with an optical emission spectrometer, resulting in 'glow discharge optical emission spectrometry' (GD-OES) (*e.g.*, ref. 7 and 8). Further, the atoms of the cathode material can also be probed directly by an external light source, making 'glow discharge atomic

†Presented at the 1999 European Winter Conference on Plasma Spectrochemistry, Pau, France, January 10–15, 1999.

absorption and fluorescence spectrometry' possible (GD-AAS[9] and GD-AFS[10]).

In order to minimize the effect of spectral interferences and contaminations due to reactions with the plasma gas, a high purity inert gas (mainly argon) is standardly used. The glow discharge is particularly well-suited for the analysis of solid conducting materials (*e.g.*, ref. 11 and 12), but also semiconductors (*e.g.*, ref. 13 and 14), non-conductors (*e.g.*, ref. 15 and 16), and even liquids[17] and gases,[18] can be analyzed. Moreover, owing to the concept of ablating the cathode material layer after layer, the glow discharge, especially in combination with OES, is routinely and successfully used for depth-profiling (*e.g.*, ref. 19 and 20). Various operation modes of glow discharges are used in analytical chemistry. The most frequently used and simplest one is the direct current (dc) mode, but other operation modes are becoming increasingly popular, such as the radiofrequency (rf) mode (*e.g.*, ref. 21 and 22), the milli- or microsecond pulsed mode (*e.g.*, ref. 23 and 24), the magnetron assisted[25,26] or the microwave boosted[27] glow discharge. Since the analytical application of glow discharges is generally known by analytical chemists, we will not go into more detail, but more information can be found in the above references and in two recent books about analytical glow discharge spectrometry.[7,28]

2.2 The micro-electronics industry and materials technology

This application field is the largest and probably most important one for glow discharges and related low pressure discharges.[3,29–32] Indeed, the glow discharge is used for etching, modification, pre-treatment and cleaning of surfaces, and for deposition of thin films on substrates. The two most important applications, *i.e.*, etching and deposition, will be described here in more detail.

2.2.1 Etching. In the micro-electronics industry, glow discharge plasmas are often used for etching of surfaces, in order to generate topographical patterns on chips, as an alternative to wet chemical etching.[3,33] The principle is as follows[3] (see Fig. 1): Suppose that one wishes to open a 'window' in a layer of SiO_2, to expose a feature on a silicon wafer. This can be done by applying a photoresist with an opening of the same size as the desired window [Fig. 1(a)]. Then, the oxide layer is exposed to the discharge, and the part not shielded by the photoresist is etched away [Fig. 1(b)]. Finally, the photoresist is removed [Fig. 1(c)]. An advantage of plasma etching is that the material can be etched vertically[3] [also called 'anisotropically'; see Fig. 2(a)], in contrast to wet chemical etching, where the material is always etched isotropically [see Fig. 2(b)] and a serious problem of non-uniformity can occur.

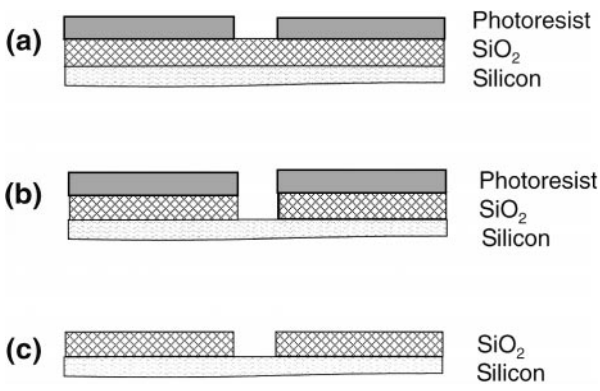

Fig. 1 Principle of etching: (a) a photoresist with suitable opening is placed on top of the material to be etched; (b) the SiO_2 material is etched away; (c) the photoresist is removed.

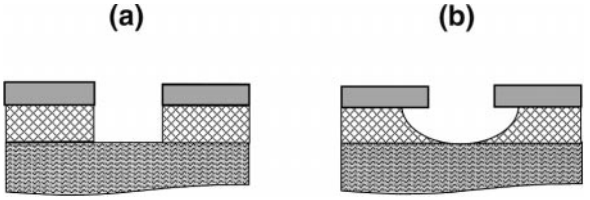

Fig. 2 Example of 'anisotropic' (or 'directional' or 'vertical') etching (a) and 'isotropic' etching (b).

Etching of surfaces by glow discharge plasmas can be performed in two distinct ways. In 'sputter-etching' the material is etched away due to the sputter-bombardment of plasma ions and atoms. This can be carried out with argon as discharge gas, and the mechanism is identical with sputtering in analytical chemistry. However, more frequently, semiconducting materials in the micro-electronics industry are being etched in so-called 'plasma-etching' (*e.g.*, ref. 34–37). A reactive plasma gas is then used, and the material is etched away due to chemical reactions at the surface. The most typical example is the etching of a Si or SiO_2 surface by a CF_4 plasma (see Fig. 3).[3] F^0 radicals from the plasma bombard the surface and react with Si to form the volatile SiF_4, which escapes from the surface, leaving a crater in the Si surface.

2.2.2 Deposition of thin films. Deposition of a layer on a substrate is not only of importance in the micro-electronics industry, but also in materials technology.[38] As with etching, deposition can also be performed in two ways.

In 'sputter-deposition' the atoms sputtered from a target arrive in the discharge plasma where they can diffuse and be deposited on a substrate (*e.g.*, ref. 39–44). The principle of sputtering is again similar to analytical chemistry, and argon is often used as the discharge gas. To enhance the sputter-deposition, this technique is often carried out in magnetron discharges, in industrial applications. Fig. 4 shows the underlying mechanisms of magnetron sputtering. The magnetron discharge consists also of two electrodes, with an electric field between them. Moreover, a magnetic field is applied at the cathode surface. The latter forces the electrons to move in closed loops around the magnetic field lines (see Fig. 4). Hence, they cover a much longer pathlength than in a glow discharge without magnetic field, giving rise to more ionization. Therefore, magnetron discharges can operate at much lower

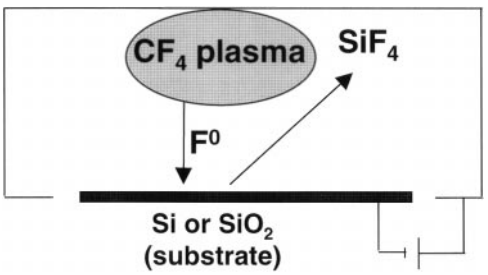

Fig. 3 Principle of plasma etching of silicon by a CF_4 plasma.

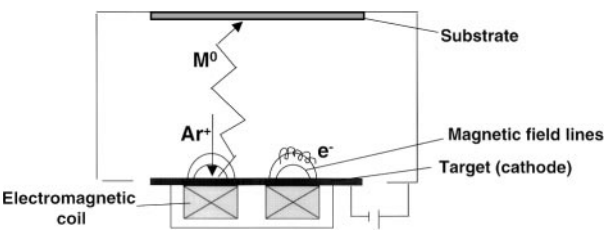

Fig. 4 Schematic diagram of a magnetron sputtering discharge.

pressures (of the order of 1–10 Pa) for the same electrical current. Similar to a simple dc glow discharge, the Ar^+ ions are accelerated to the cathode by the strong electric field, and they sputter away cathode (target) atoms. The latter arrive in the plasma and can be deposited on the substrate. The transport of the target atoms to the substrate is generally much more efficient due to the lower operating pressure of the magnetron discharge, and hence the virtual absence of scattering elastic collisions.

In addition, 'plasma-deposition or plasma enhanced chemical vapor deposition (PE-CVD)' is often applied for important industrial applications. The discharge gas is then a reactive gas, and due to chemical reactions in the plasma (ionization, dissociation, …) various kinds of radicals and ions are formed, which can diffuse to a substrate and be deposited (due to chemical surface reactions). A common example is the deposition of diamond-like-carbon layers (DLC, or amorphous hydrogenated carbon; a-C:H) in a CH_4–H_2 plasma, for the formation of protective hard coatings, to reduce wear and/or friction, or for anti-sticking purposes (*e.g.*, ref. 45–47). Another application is the deposition of amorphous hydrogenated silicon layers (a-Si:H) from a SiH_4–H_2 plasma, used for the fabrication of thin film transistors, xerographic materials, solar cells, *etc.* (*e.g.*, ref. 48–50). The principle of the deposition of DLC layers is illustrated in Fig. 5. It is usually carried out in a plasma containing a mixture of CH_4 and H_2. However, in addition to these two gases, also other species are present in the plasma, such as electrons, and various kinds of ions and radicals, which are mainly formed by electron impact ionization and dissociation of CH_4 and H_2. These species can be deposited on the substrate, and lead to the formation of a DLC film. It is suggested that the CH_3 radical is the most important film-growing species for DLC layers.[51]

Various types of discharges are nowadays being used for the deposition and etching of surfaces. In addition to the most simple direct current (dc) glow discharge, the capacitively coupled radiofrequency (CC rf) glow discharge is also popular, especially for the etching and deposition of non-conducting materials. However, the latter operation mode is not so advantageous for up-scaling to larger reactors (which is a new tendency in materials technology), due to the high cost of large rf-generators. Therefore, the pulsed dc operation mode, and the (lower than rf-frequency) alternating current (ac) discharges are attracting increasing interest. As mentioned before, also the magnetron discharges are frequently used for industrial applications of thin film deposition. Finally, some new, high plasma density sources are becoming more and more popular, of which the electron cyclotron resonance (ECR) source and the inductively coupled plasma (ICP) are the most well-known. In the ECR source (*e.g.*, ref. 34, 36 and 52), a magnetic field is applied to the discharge, which forces the electrons to cycle around the magnetic field lines with a certain frequency. When microwave energy of the same frequency (*i.e.*, 2.54 GHz) is applied to the discharge, a resonance effect occurs, which leads to very efficient energy-pumping into the plasma. In the ICP source (*e.g.*, ref. 35, 53 and 54), the rf-energy is not capacitively but inductively coupled to the plasma, by means of an external coil. The principle of inductive coupling is, hence, similar to the analytical ICPs, but the essential difference is the pressure. Indeed, in contrast to the analytical ICPs, the technological ICPs operate in the pressure regime of a few mTorr, and are hence far from thermodynamic equilibrium, which is in fact a common characteristic of all low pressure discharges.

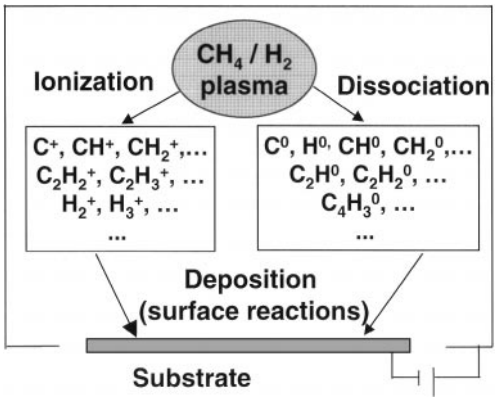

Fig. 5 Schematic diagram of plasma enhanced chemical vapor deposition (PE-CVD) for the deposition of diamond-like-carbon (DLC).

2.3 Lasers

Various types of lasers are also based on glow discharge plasmas. The lasers most closely related to the analytical glow discharges are the so-called 'metal vapor ion lasers' (*e.g.*, ref. 55–62). An inert gas (helium, neon or argon) is used as the discharge gas, and atoms of a transition metal are introduced into the discharge, either by evaporation or by sputtering as in analytical chemistry. Typical examples are He–Cd, He–Zn, He–Hg and Ne–Cu lasers. Population inversion, necessary for laser action, is attained by asymmetric charge transfer between the discharge gas ions and the sputtered atoms (*e.g.*, $Ne^+ + Cu^0 \rightarrow Ne^0 + Cu^+$). The discharge type is generally a dc hollow cathode discharge.

Another type of glow discharge with laser properties, based on a neon–copper mixture, is the 'copper vapor laser' (*e.g.*, ref. 63–67). The discharge type is the positive column of a dc or pulsed discharge. In this case, population inversion for laser action is caused by simple electron impact excitation. The latter process is much more efficient to the Cu^0 $3d^{10}$ $4p$ $^2P_{1/2}$ and $^2P_{3/2}$ levels than to the lower lying $3d^9$ $4s^2$ $^2D_{3/2}$ and $^2D_{5/2}$ levels, which gives population inversion of these levels, resulting in Cu atomic laser lines at 510.6 and 578.2 nm.

Further, laser action can also be reached in other discharge types, of which the excimer lasers[68,69] (*e.g.*, Ar_2, ArF, XeCl, KrF, …) and the CO_2 lasers[70] are two common examples.

2.4 Lamps

Since the glow discharge emits light due to excitation and subsequent radiative decay to lower levels, it is clear that it is also being used for lighting purposes,[71–73] *e.g.*, the fluorescent lamps, the neon lamps (in illuminated advertisements) and the xenon lamps (in modern cars). Also worthy of mention are the new types of electrodeless induction lamps, which are atmospheric pressure ICPs (*e.g.*, ref. 74–78). An example of the Philips QL lamp, with the plasma outside the induction coil instead of inside, is shown in Fig. 6.[77,78] It consists of a coil of 15 windings with a ferrite core (the antenna) surrounded by a bulb. An rf-generator (not depicted) feeds the coil with an alternating current of 2.65 MHz and an amplitude of typically 1 A. This induces a plasma current of approximately 10 A. The power delivered by the rf-generator is held constant at 80 W. The bulb contains a mixture of argon and mercury.

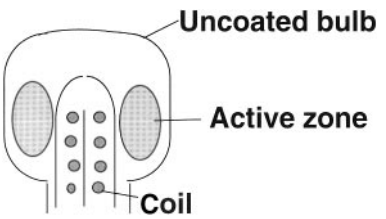

Fig. 6 Schematic diagram of the Philips QL lamp.[78]

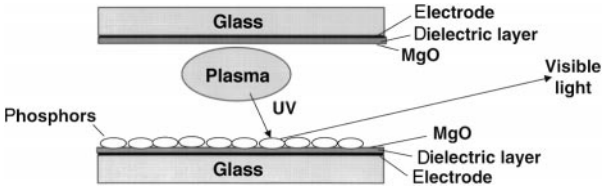

Fig. 7 Schematic diagram of a micro-discharge for plasma display panels.

As in all fluorescent lamps, mercury is the active species in the lamp, *i.e.*, most of the inelastic collisions take place between free electrons and mercury atoms. The argon has to be present as a buffer gas; otherwise the gas pressure would be too low and electrons and ions would easily diffuse to the wall, where recombination takes place. The great advantage of this lamp type (as well as of the other types of electrodeless lamps) is that reactions between the electrodes and the plasma are avoided, leading to much longer lifetimes of the lamp.

2.5 Displays

Another growing field of application is the display technology. The so-called 'plasma display panels (PDPs)' (*e.g.*, ref. 79–82), which are attracting increasing interest as television screens, are based on several micro-discharges. Such a micro-discharge consists of two electrodes both covered by a dielectric layer and a MgO layer, and separated by, *e.g.*, 0.1 mm. Two kinds of electrode designs are now being used. In the 'matrix-electrode design', a number of line and column electrodes, placed orthogonally to each other, are deposited on two parallel glass plates. A discharge is formed at each intersection of the line and column electrodes. In the 'coplanar-electrode design', two perpendicular sets of parallel electrodes are deposited on the glass plates, but the discharges now occur between two electrodes on the same plate, and can be triggered by the electrode on the other plate. The dielectric barriers are used to avoid optical and electrical interaction between neighboring cells. A typical discharge gas is a mixture of Xe–Ne (in a ratio of 10 : 90) at a pressure of *ca.* 500 Torr. The discharge voltage is typically of the order of 200 V, and is applied as an alternating current (ac) square wave voltage. The latter is required by the dielectric layers on top of the electrodes, to avoid charging-up of the electrodes. One of the two electrodes is also covered with phosphors, which convert the UV light emitted by the discharge plasma into visible light. A picture element in a display consists of three discharge cells next to each other, coated with phosphors in the three fundamental colors. A schematic diagram of such a micro-discharge in the matrix-electrode design is shown in Fig. 7.

Another type of display making use of plasmas is the plasma activated liquid crystal (PALC) display. In contrast to the PDPs, the plasma is here not used as a light-emitter, but is applied as an electrical switch for the liquid crystal, because it can conduct electrical current.

3 Modeling approaches

In order to improve the results in all these application fields, a good insight into the discharge processes is desirable. This can be obtained by measurements in the plasma (*i.e.*, plasma diagnostics), but also by mathematical modeling. A number of different modeling approaches exist for the description of glow discharges.

In the 'analytical model',[83,84] the plasma quantities are calculated as a function of discharge conditions (pressure, voltage, current, power) by analytical scaling laws. This gives a rapid prediction of the glow discharge, but the approximations made to deduce the scaling laws are often only valid for certain conditions.

In the 'fluid model',[85,86] the plasma species are considered as a fluid, in equilibrium with the electric field. They are described with the first (three) moments of the Boltzmann equation, *i.e.*, the particle continuity, momentum balance, and energy balance equations. When this model is used for charged plasma species, the above-mentioned equations are often coupled to Poisson's equation, to obtain a self-consistent electric field distribution throughout the discharge. Such model calculations are also fairly fast (although it can be tricky to solve the coupled non-linear differential equations), but it is also only an approximation. Indeed, the assumption of equilibrium with the local electric field is not valid for the fast electrons in the discharge, because they gain more energy from this field than they lose by collisions.

In the 'Boltzmann model',[87,88] the non-equilibrium behavior of the particles is accounted for, and they are described with the full Boltzmann transport equation, with different terms describing the energy gain from the electric field and the energy loss due to collisions. However, a disadvantage of this model is that it becomes mathematically very complicated, especially when the glow discharge is being described in more than one dimension.

In the 'Monte Carlo model',[89,90] the plasma species are treated as separate particles. Their trajectory in the electric field is calculated by Newton's laws and the collisions (*i.e.*, occurrence and kind of collision, and new energy and direction after collision) are handled by random numbers. By following in this statistical way a large number of particles, the glow discharge can be simulated. This model is the most accurate one, because it describes the behavior of the separate particles explicitly. Moreover, it is mathematically very simple. However, in order to reach satisfactory statistics, a long calculation time is required, especially when slow particles (such as slow electrons and ions, or neutral atoms) are being described. Moreover, this model requires a certain electric field distribution as input value, and hence it does not give a self-consistent description of the glow discharge.

This problem is overcome in the 'particle-in-cell model',[91,92] which couples a Monte Carlo calculation of the trajectory and collisions of the particles, to the Poisson equation, in order to obtain a self-consistent electric field distribution. This is an additional advantage, next to the inherent advantages of the Monte Carlo model (*i.e.*, being accurate and simple). However, it requires an even longer calculation time than a pure Monte Carlo model, because (i) a large number of particles have to be followed for valid statistics, and (ii) a very small time-step is needed for the solution of the Poisson equation.

Hence, each of the models has its particular advantages and disadvantages. Therefore, 'hybrid models'[93–95] are sometimes used, which consist of an accurate but computationally intensive model (*e.g.*, Monte Carlo) for some plasma species (*e.g.*, fast electrons) and a model which yields fast calculations but is only approximate (*e.g.*, fluid model) for other species (*e.g.*, neutral atoms, for which the approximation is valid). Hence, this model has, in principle, the advantages of both models (*i.e.*, being both accurate and making the calculations reasonably fast) and no real disadvantages (although it can still require a fairly long calculation time). It is interesting to note that typical computation times can vary from a few minutes (for the simple analytical approaches) to several days (for the hybrid Monte Carlo–fluid models and the particle-in-cell methods).

Finally, another model worthy of mention is the so-called 'collisional-radiative model'[96,97] used for plasma atoms or ions in excited levels. It is, actually, a kind of fluid model, consisting of coupled continuity (or balance) equations with various production and loss terms. Because the production and loss

processes of these excited levels are of a collisional or radiative nature, this model is called a collisional-radiative model.

In the literature, a large number of models have been presented. Most of these models apply to discharges used for etching and deposition (*e.g.*, ref. 83–89 and 91–94). Apart from obtaining a better general understanding, which is always one of the aims of modeling, the 'uniformity issue' in the case of etching is an important incentive for these models. It is, indeed, important to have anisotropic etching [see Fig. 2(a)], in order to obtain perfectly vertical crater walls, which are uniform across the entire wafer. Moreover, for the deposition of thin layers in materials technology, up-scaling to larger reactors is nowadays a real challenge. This up-scaling is still often carried out by trial-and-error. However, building larger reactors by trial-and-error is very expensive and often time consuming. Therefore, modeling can present a solution, *i.e.*, in the model, the effect of a larger cell geometry is predicted prior to building the new reactor cell. NIST, for example, has an entire program devoted to the establishment of etching/deposition system standardization.

Further, because the plasma display panel technology is one of the promising new applications of glow discharges, a lot of modeling is now also devoted to this type of micro-discharge.[98] The aim is to study effects of the geometry such as electrical or optical interaction between adjacent cells (cross-talk problems in high resolution displays) or the sensitivity of the display to defects such as electrode misalignment. Another main challenge is the improvement of the luminous efficiency, which is at the moment still rather low.[98]

For the prediction of optimization of the light intensity and luminous efficiency of lamps, some models are also being developed for this application (*e.g.*, ref. 74–77 and 99). These models consist, for example, of collisional-radiative models, to describe the behavior of excited levels and hence to calculate the light emission. Similarly, some models are also being developed for the description of gas discharge lasers (*e.g.*, ref. 66, 67, 90, 95 and 97), in order to optimize the laser output power and laser gain.

Finally, glow discharges used for analytical purposes have also recently become the subject of modeling (*e.g.*, ref. 100–110), for example, for understanding variations in relative sensitivity factors in GDMS,[111] for the calculation of ion intensities and optical emission intensities,[112,113] for crater optimization in GD depth-profiling,[114] and for the prediction of the effect of the cell geometry.[115,116] In the next section, we will briefly present our own hybrid model set-up for analytical glow discharges.

Table 1 Species assumed to be present in the plasma, and models used to describe these species

Species	Model
Thermal argon gas atoms	No model, assumed uniformly distributed
Fast electrons	Monte Carlo model (entire discharge)
Slow electrons	Fluid model (entire discharge)
Argon ions	Fluid model (entire discharge) Monte Carlo model (cathode dark space)
Fast argon atoms	Monte Carlo model (cathode dark space)
Argon atoms in excited levels	Collisional-radiative model (entire discharge)
Sputtered atoms: thermalization	Monte Carlo model (entire discharge)
Sputtered atoms +ions, in ground state+excited levels	Collisional-radiative model (entire discharge)
Sputtered ions	Monte Carlo model (cathode dark space)

Table 2 Typical quantities calculated for a dc glow discharge

Fundamental plasma quantities:
- Densities, fluxes and energies of the various plasma species
- Information about collision processes in the plasma
- Information about interaction at the cell walls (*e.g.*, sputtering)
- Potential and electric field distributions in the plasma
- Current–voltage–pressure characteristics

Quantities of direct importance for analytical applications:
- Optical emission intensities and ion intensities
- Explanation of variations in relative sensitivity factors
- Crater profiles and erosion rates
- Prediction of effect of cell geometry

4 Hybrid model of analytical glow discharges

In previous years, we have developed a comprehensive hybrid model for a dc glow discharge in argon, and a similar model for an rf discharge in argon is currently under development.

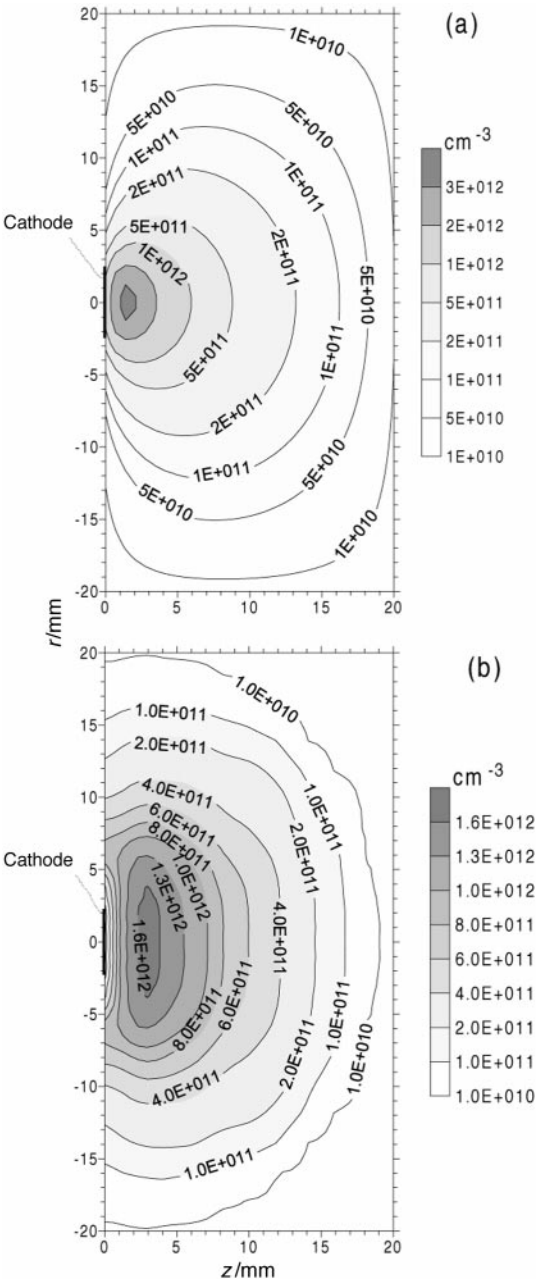

Fig. 8 Sputtered tantalum atom densities, calculated (a) and measured by laser induced fluorescence (b), for a six-way cross glow discharge, at 1000 V, 1 Torr and 2 mA (reprinted from ref. 117 with permission from Elsevier Science).

This hybrid model consists of various sub-models (*i.e.*, Monte Carlo, fluid and collisional-radiative models) for the various species present in the glow discharge. Table 1 gives an overview of the species described in the hybrid model and the sub-models used to describe these species. The Monte Carlo models are developed in three dimensions; the fluid and collisional-radiative models are only two-dimensional, because, owing to the cylindrical symmetry of the discharge cells under consideration, the three dimensions in the equations could be reduced to two dimensions (axial and radial direction). More information about these models can be found, *e.g.*, in ref. 100–105 and 107–110. In the following, some results of the models will be presented.

4.1 Modeling of a dc glow discharge in argon

The typical quantities that we have calculated for a dc glow discharge are summarized in Table 2. A few examples will be outlined here. Fig. 8(a) shows the calculated sputtered tantalum atom density for a six-way cross glow discharge at 1 Torr, 1000 V and 2 mA. A schematic picture of a six-way cross set-up can be found in ref. 117. The black thick line at $z=0$ and around $r=0$ symbolizes the cathode; the other figure borders represent the cell walls which are at anode potential. To check the validity of this model, the calculated results were compared with experimental data, measured by laser induced fluorescence spectrometry [see Fig. 8(b)].[117] In general, there is satisfactory qualitative and quantitative agreement (only a factor of 2 difference, which does not exceed the expected uncertainties of both modeling and experimental results).

Fig. 9(a) shows a calculated optical emission spectrum of the argon atoms in a glow discharge at 1 Torr, 1000 V and 2 mA.[112] The spectrum is clearly dominated by peaks in the 700–1000 nm region, *i.e.*, the so-called red lines. Also, the experimental Ar(I) spectrum is clearly dominated by these red lines, as follows from Fig. 9(b)[112] (adopted from tabulated values for a hollow cathode glow discharge at 150 mA and 1 Torr[118]). Although the discharge conditions of the calculated and experimental results are significantly different, and although the experimental data were not corrected for spectrometer response, similar trends in the relative line intensities in both spectra are observed.

Another calculated quantity, of interest for GD depth-profiling, is the crater profile due to sputtering at the cathode, as is presented in Fig. 10(a) (calculated for the VG9000 flat cell, at 0.75 Torr, 800 V and 4 mA).[114] The calculated crater is much deeper at the sides than in the center, and the crater walls are not completely vertical. Moreover, there appears to be some accumulation of sputtered material just outside the crater. The calculated crater is a good prediction of the experimental crater at similar discharge conditions and for the same cell geometry, as is presented in Fig. 10(b).[119] Indeed, also, the measured crater is much deeper at the sides than in the center, has non-vertical crater walls and there is some accumulation of sputtered material outside the crater. Also, the absolute values of the crater depth are in satisfactory agreement. This example illustrates that the model is able to reproduce more or less the experimental crater profiles. Hence, the effect of the cell geometry and discharge conditions on the crater profile to be expected, can, in principle, be predicted.

Finally, a last example for the dc discharge, to illustrate the

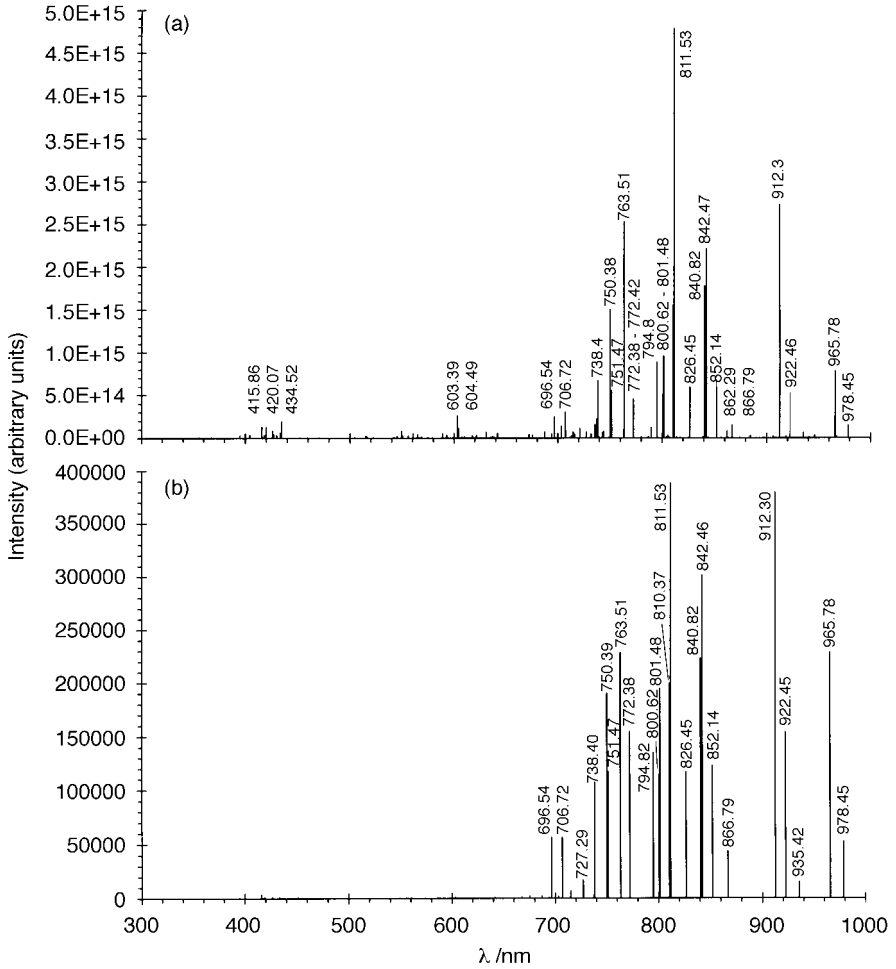

Fig. 9 Argon atomic optical emission spectra, calculated for a six-way cross glow discharge at 1000 V, 1 Torr and 2 mA (a), and measured in a hollow cathode glow discharge at 150 mA and 1 Torr (b)[118] (reprinted from ref. 112 with permission of Elsevier Science).

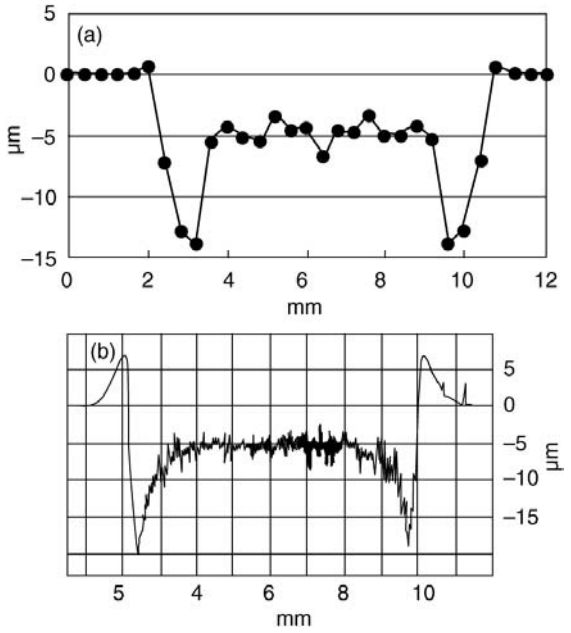

Fig. 10 Crater profile due to sputtering at the cathode, calculated for the VG9000 glow discharge cell at 800 V, 0.75 Torr and 4 mA (a),[114] and measured for the same cell at 750 V and 3 mA (b).[114,119]

ability of the models to predict the effect of the cathode geometry, is presented in Fig. 11(a) and (b).[116] They show the calculated copper ion density profile in a cell with a flat or pin-type cathode. In the flat-cathode cell, the maximum copper ion density is reached at the cell axis, at about 5 mm from the cathode. In the pin-cathode cell, the maximum is not reached at the cell axis, but in a ring around the pin-cathode, at about 5 mm from the pin surface. This rather distinct distribution is in excellent agreement with the calculation results of Fiala and co-workers.[106] From this, also the ion currents to the mass spectrum can be calculated and compared for the flat-cathode and pin-cathode cells. Of course, not only the effect of the cathode geometry, but also of the cell geometry, can be obtained from the model calculations. Hence, the models can be useful for new cell design.

4.2 Modeling of an rf discharge in argon

In principle, the same quantities that have been calculated for a dc glow discharge can also be obtained for an rf discharge, and such a hybrid model is currently under development. At present, the electrons, argon ions and fast argon atoms have been described by a combination of Monte Carlo and fluid models. The quantities that have been calculated up to now comprise the potential and electric field distributions, the rf and dc bias voltages, the densities, fluxes and energy distributions of the electrons, argon ions and argon atoms, information about collision processes in the plasma, *etc*. Some selected examples will be illustrated here.

Fig. 12 shows the potential at the rf-electrode (*i.e.*, the sample) as a function of time in the rf-cycle, at typical rf-GD-OES discharge conditions (5 Torr gas pressure, 10 W power). It is negative (*i.e.*, plays the role of cathode) during most of the rf-cycle, due to a negative dc-bias (V_{dc}). The latter is caused by the difference in area of the rf-powered electrode (*i.e.*, sample) and the grounded electrode (*i.e.*, cell walls). The potential at the rf-electrode is only positive around $\pi/2$. This calculated waveform is in excellent qualitative agreement with experimentally measured waveforms.[120] The plasma potential is also plotted as a function of time in the rf-cycle in Fig. 12 (V_{plasma}; dashed line). It is equal to the potential at the

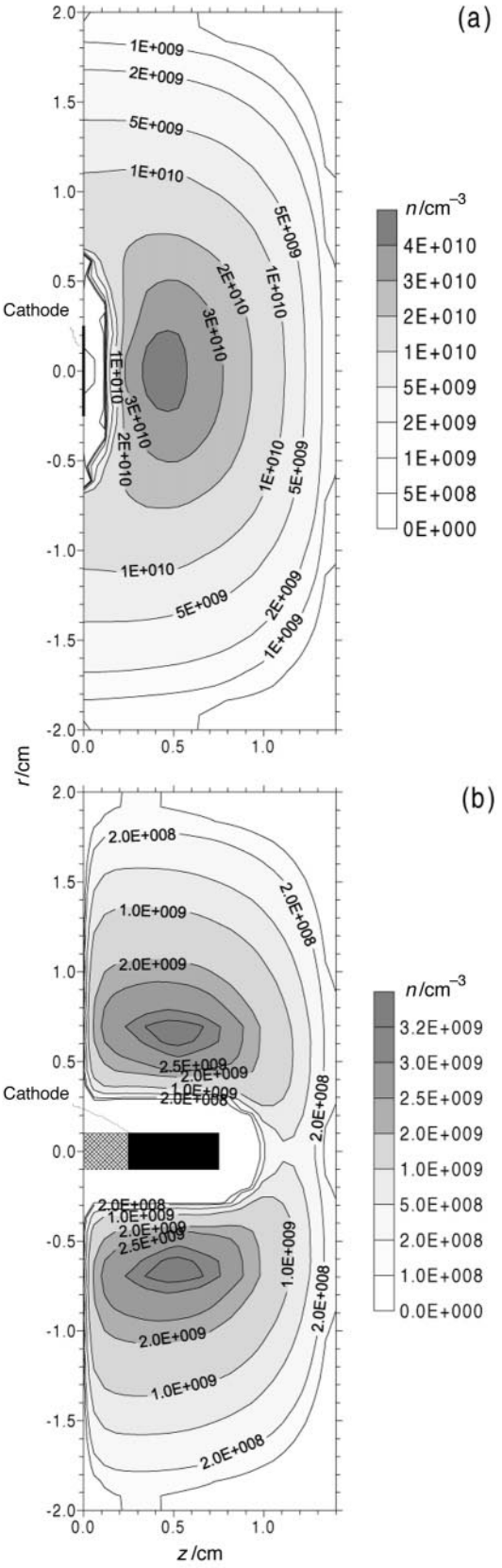

Fig. 11 Copper ion densities, calculated for a cell with flat-type (a) and pin-type (b) cathode, at 1000 V, 2.2 mA, 1 and 0.7 Torr, respectively (reprinted from ref. 116 with permission from Elsevier Science).

rf-electrode around $\pi/2$, and decreases to a nearly constant value of about 40 V during most of the rf-cycle.

The two-dimensional potential distribution, at four different times in the rf-cycle, is illustrated in Fig. 13. The rf-powered

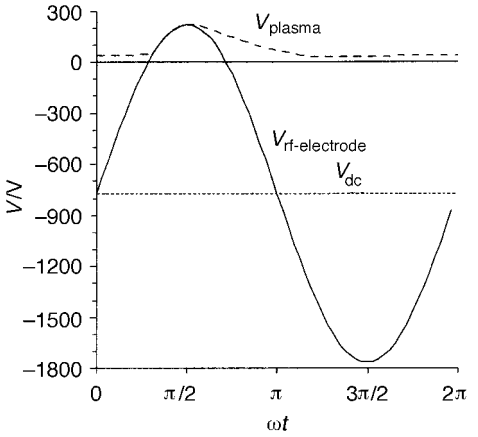

Fig. 12 Potential at the rf-electrode ($V_{rf\text{-}electrode}$; solid line), plasma potential (V_{plasma}; dashed line), and dc bias voltage (V_{dc}; dotted line), as a function of time in the rf-cycle, at 5 Torr and 10 W.

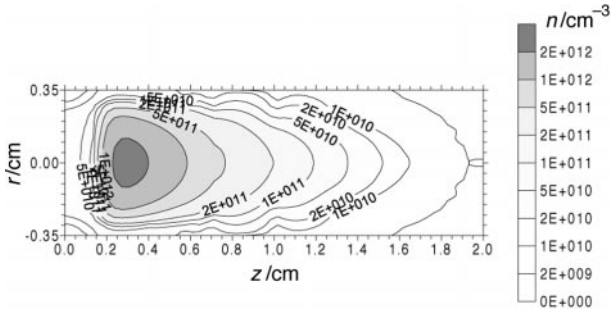

Fig. 14 Two-dimensional argon ion density profile throughout the discharge (constant during the entire rf-cycle) at 5 Torr and 10 W.

electrode is at the left side of the figure, whereas the other boundaries of the figure represent the grounded electrode. At $\pi/2$, the potential is positive at the rf-electrode, and also throughout the largest part of the cell. It goes, of course, to zero at the grounded cell walls. At the other times in the rf-cycle, the potential is very negative at the rf-electrode, as was expected already from Fig. 12. It crosses zero at about 1 mm from the rf-electrode and is positive in the remainder of the plasma. The position where the potential crosses the zero line is defined here as the interface between the rf-sheath and the bulk plasma. Except at $\pi/2$, the rf potential distribution resembles very much a dc potential distribution (see, *e.g.*, ref. 104 and 115).

Also, the rf argon ion density profile, depicted in Fig. 14, is very similar to a dc argon ion density profile (*e.g.*, ref. 104 and 115), especially when calculated for the same cell geometry. It is low in the rf-sheath, and reaches a maximum at about 3 mm from the rf-electrode (*i.e.*, in the beginning of the bulk plasma) and then it returns to low values at the anode walls. More information about our recent calculation results for an rf discharge in argon can be found in ref. 121 and 122.

5 Conclusion

We have tried to illustrate that numerical modeling of glow discharges (and fundamental research in general) is an interesting field of study, because it gives a better insight into the complex plasma processes, and it can improve the analytical capabilities of the glow discharge. Moreover, glow discharges are increasingly being applied in fields other than analytical chemistry, *i.e.*, in the micro-electronics industry, as lasers, light sources, displays, *etc*. Since the number of applications of glow discharges is still growing [*e.g.*, also for environmental applications, such as the plasma abatement of perfluoro compounds (PFCs), the plasma decomposition of NO_2, the exhaust gas treatment by dielectric barrier discharges, for ozone generation in corona streamers, *etc.*], and since the existing applications (especially in the micro-electronics industry and materials technology, and for lasers and plasma displays) are becoming increasingly important, we can conclude that glow discharges are indeed very exciting plasmas with a bright future!

We expect that future efforts will be directed, among others, to developing new discharge configurations and optimizing existing types, with still higher plasma densities, better uniformity and higher efficiencies, for still better application results. To reach this, model predictions will remain very powerful tools, both accurate models which can describe specific effects and details, but also more simple models which

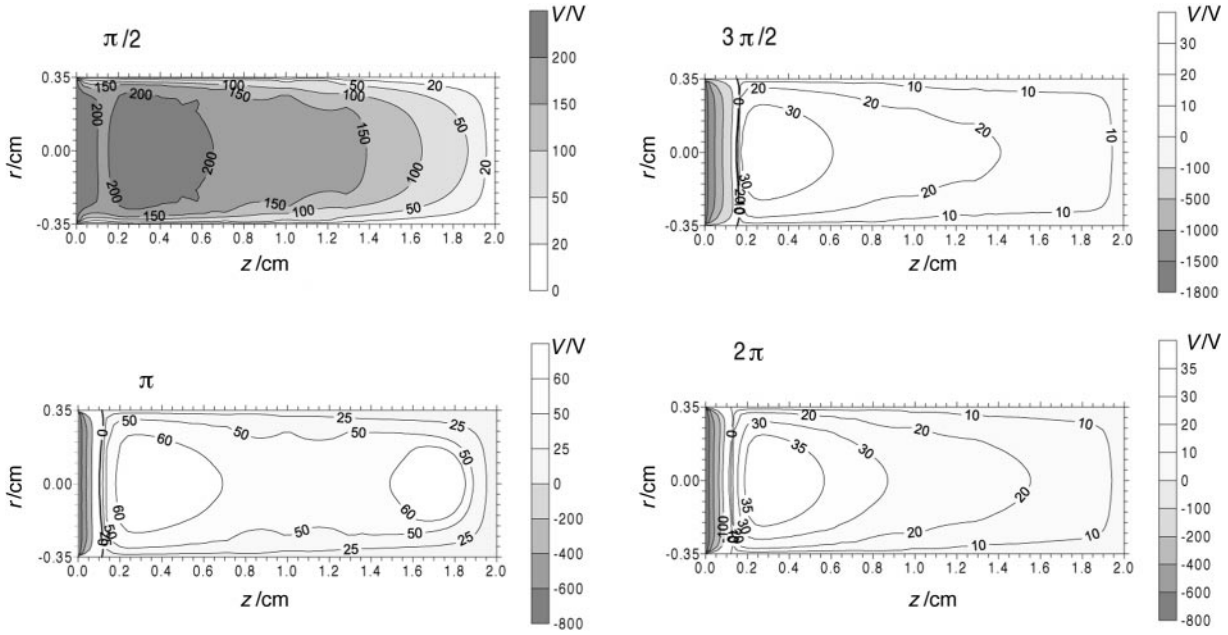

Fig. 13 Two-dimensional potential distributions throughout the discharge, at four times in the rf-cycle, at 5 Torr and 10 W.

can be employed *e.g.*, by industrial users, to give a rapid prediction of the plasma behavior.

Acknowledgements

A. Bogaerts is indebted to the Flemish Fund for Scientific Research (FWO) for financial support. Moreover, she thanks Professor R. Gijbels for his continued interest and support. Finally, she acknowledges financial support from the Federal Services for Scientific, Technical and Cultural Affairs (DWTC/SSTC) of the Prime Minister's Office through IUAP-IV (Conv. 4/10).

References

1 M. J. Druyvenstein and F. M. Penning, *Rev. Mod. Phys.*, 1940, **12**, 87.
2 G. Francis, in *Encyclopedia of Physics*, *Volume XXII: Gas Discharges II*, ed. S. Flügge, Springer-Verlag, Berlin, 1956, pp. 53–208.
3 B. Chapman, *Glow Discharge Processes*, Wiley, New York, 1980.
4 F. F. Chen, *Plasma Physics and Controlled Fusion*, *Volume 1: Plasma Physics*, Plenum, New York, 1984.
5 W. W. Harrison and B. L. Bentz, *Prog. Anal. Spectrosc.*, 1988, **11**, 53.
6 W. W. Harrison, K. R. Hess, R. K. Marcus and F. L. King, *Anal. Chem.*, 1986, **58**, 341A.
7 *Glow Discharge Optical Emission Spectrometry*, ed. R. Payling, D. G. Jones and A. Bengtson, Wiley, Chichester, 1997.
8 A. Bengtson, *J. Anal. At. Spectrom.,* 1996, **11**, 829.
9 K. Song, E. Jung, H. Cha, J. Lee, M.-J. Kim and S. C. Lee, *J. Anal. At. Spectrom.*, 1998, **13**, 301.
10 W. O. Walden, W. W. Harrison, B. W. Smith and J. D. Winefordner, *J. Anal. At. Spectrom.*, 1994, **9**, 1039.
11 N. Jakubowski, D. Stuewer and W. Vieth, *Anal. Chem.*, 1987, **59**, 1825.
12 C. Venzago, L. Ohanessian-Pierrard, M. Kasik, U. Collisi and S. Baude, *J. Anal. At. Spectrom.*, 1998, **13**, 189.
13 A. P. Mykytiuk, P. Semeniuk and S. Berman, *Spectrochim. Acta Rev.*, 1990, **13**, 1.
14 R. Jäger, A. I. Saprykin, J. S. Becker, H.-J. Dietze and J. A. C. Broekaert, *Mikrochim. Acta*, 1997, **125**, 41.
15 S. De Gendt, W. Schelles, R. Van Grieken and V. Mueller, *J. Anal. At. Spectrom.*, 1995, **10**, 681.
16 W. Schelles and R. Van Grieken, *Anal. Chem.*, 1997, **69**, 2931.
17 N. Jakubowski, D. Stuewer and G. Toelg, *Spectrochim. Acta*, *Part B*, 1991, **46**, 155.
18 D. C. Duckworth, C. M. Barshick, D. H. Smith and S. A. McLucky, *Anal. Chem.*, 1994, **66**, 92.
19 F. Prässler, V. Hoffmann, J. Schumann and K. Wetzig, *J. Anal. At. Spectrom.*, 1995, **10**, 677.
20 A. Bengtson and S. Hanstrom, *J. Anal. At. Spectrom.*, 1998, **13**, 437.
21 D. C. Duckworth and R. K. Marcus, *Anal. Chem.*, 1989, **61**, 1879.
22 M. Parker and R. K. Marcus, *Spectrochim. Acta*, *Part B*, 1995, **50**, 617.
23 W. Hang, C. Baker, B. W. Smith, J. D. Winefordner and W. W. Harrison, *J. Anal. At. Spectrom.*, 1997, **12**, 143.
24 W. W. Harrison, W. Hang, X. Yan, K. Ingeneri and C. Schilling, *J. Anal. At. Spectrom.*, 1997, **12**, 891.
25 M. J. Heintz, J. A. C. Broekaert and G. M. Hieftje, *Spectrochim. Acta*, *Part B*, 1997, **52**, 579.
26 A. I. Saprykin, J. S. Becker and H.-J. Dietze, *Fresenius' J. Anal. Chem.*, 1996, **355**, 831.
27 F. Leis and E. B. M. Steers, *Spectrochim. Acta*, *Part B*, 1994, **49**, 289.
28 *Glow Discharge Spectroscopies*, ed. R. K. Marcus, Plenum, New York, 1993.
29 D. A. Glocker and S. I. Shah, *Handbook of Thin Film Process Technology*, IOP Publishing, Bristol, 1995.
30 M. A. Lieberman and A. J. Lichtenberg, *Principles of Plasma Discharges and Materials Processing*, Wiley, New York, 1994.
31 A. Grill, *Cold Plasmas in Materials Fabrication*, IEEE Press, New York, 1993.
32 D. B. Graves, *IEEE Trans. Plasma Sci.*, 1994, **22**, 31.
33 D. M. Manos and D. L. Flamm, *Plasma Etching: An Introduction*, Academic Press, New York, 1989.
34 J. Asmussen, *J. Vac. Sci. Technol. A*, 1989, **7**, 883.
35 J. Hopwood, *Plasma Sources Sci. Technol.*, 1992, **1**, 109.
36 N. Sato, S. Iizuka, Y. Nakagawa and T. Tsukada, *Appl. Phys. Lett.*, 1993, **62**, 1469.
37 S. Samukawa and T. Nakano, *J. Vac. Sci. Technol. A*, 1996, **14**, 1002.
38 B. Lux, R. Haubner, M. Griesser and M. Grasserbauer, *Mikrochim. Acta*, 1997, **125**, 197.
39 M. Yamashita, *J. Vac. Sci. Technol. A*, 1989, **7**, 151.
40 S. M. Rossnagel and J. Hopwood, *J. Vac. Sci. Technol. B*, 1994, **12**, 449.
41 M. Kadota, T. Kasanammi and M. Minakata, *Jpn. J. Appl. Phys.*, 1992, **31**, 3013.
42 G. Este and W. D. Westwood, *J. Vac. Sci. Technol. A*, 1988, **6**, 1845.
43 S. M. Rossnagel, D. Mikalsen, H. Kinoshita and J. J. Cuomo, *J. Vac. Sci. Technol. A*, 1991, **9**, 261.
44 H. Haberland, M. Karrais, M. Mall and Y. Thurner, *J. Vac. Sci. Technol. A*, 1992, **10**, 3266.
45 Y. Catherine, *Diamond and Diamond-like Films and Coatings*, Plenum, New York, 1991.
46 P. Koidl, Ch. Wild, B. Dischler, J. Wagner and M. Ramsteiner, *Mater. Sci. Forum*, 1989, **52–53**, 41.
47 J. Robertson, *Surf. Coat. Technol.*, 1992, **50**, 185.
48 E. Bertran, S. N. Sharma, G. Viera, J. Costa, P. St'ahel and P. Cabarrocas, *J. Mater. Res.*, 1998, **13**, 2477.
49 K. Tanaka and A. Matsuda, *Mater. Sci. Rep.*, 1987, **2**, 139.
50 H. Fritzsche, *Sol. Energy Mater.*, 1980, **3**, 447.
51 W. Möller, *Appl. Phys. A*, 1993, **56**, 527.
52 M. Misina, Y. Setsuhara and S. Miyake, *Jpn. J. Appl. Phys.*, 1997, **36**, 3629.
53 J. Hopwood, C. R. Guarnieri, S. J. Whitehair and J. J. Cuomo, *J. Vac. Sci. Technol. A*, 1993, **11**, 147.
54 J. A. O'Neill, M. S. Barnes and J. H. Keller, *J. Appl. Phys.*, 1993, **73**, 1621.
55 W. T. Silvast and M. B. Klein, *Appl. Phys. Lett.*, 1970, **17**, 400.
56 G. J. Collins, R. C. Jensen and W. R. Bennet, *Appl. Phys. Lett.*, 1971, **18**, 282.
57 L. Csillag, M. Janossy, K. Rozsa and T. Salamon, *Phys. Lett. A*, 1974, **50**, 547.
58 J. R. McNeil, W. L. Johnson, G. J. Collins and K. B. Persson, *Appl. Phys. Lett.,* 1976, **29**, 172.
59 D. C. Gerstenberger, R. Solanki and G. J. Collins, *IEEE J. Quantum Electron.*, 1980, **16**, 820.
60 K. Rozsa, *Z. Naturforsch.,* 1980, **35**, 649.
61 K. A. Peard, Z. Donko, K. Rozsa, L. Szalai and R. C. Tobin, *IEEE J. Quantum Electron.*, 1994, **30**, 2157.
62 I. G. Ivanov, E. I. Latush and M. F. Sem, *Metal Vapour Ion Lasers: Kinetic Processes and Gas Discharges*, Wiley, Chichester, 1996.
63 D. W. Coutts and J. A. Piper, *IEEE J. Quantum Electron.*, 1992, **28**, 1761.
64 M. H. Knowles and C. E. Webb, *Opt. Lett.*, 1993, **18**, 607.
65 A. C. J. Glover, E. K. Illy and J. A. Piper, *IEEE J. Sel. Top. Quantum Electron.*, 1995, **1**, 830.
66 R. J. Carman, D. J. W. Brown and J. A. Piper, *IEEE J. Quantum Electron.*, 1994, **30**, 1876.
67 R. J. Carman, *J. Appl. Phys.*, 1997, **82**, 71.
68 W. M. Hughes, J. Shannon and R. Hunter, *Appl. Phys. Lett.*, 1974, **24**, 488.
69 W.-G. Wrobel, H. Röhr and K.-H. Steuer, *Appl. Phys. Lett.*, 1980, **36**, 113.
70 A. Cenian, A. Chernukho, P. Kukiello, R. Zaremba, V. Borodin and G. Sliwinski, *J. Phys. D*, 1997, **30**, 1103.
71 J. F. Waymouth, *Electric Discharge Lamps*, MIT Press, Boston, MA, 1971.
72 W. Elenbaas, *Light Sources*, McMillan, London, 1972.
73 J. J. de Groot and J. A. J. M. van Vliet, *The High-pressure Sodium Lamp*, Philips Technical Library, The Netherlands, 1986.
74 J. W. Denneman, *J. Phys. D*, 1990, **23**, 293.
75 G. G. Lister and M. Cox, *Plasma Sources Sci. Technol.*, 1992, **1**, 67.
76 R. B. Piejak, V. A. Godyak and B. M. Alexandrovich, *Plasma Sources Sci. Technol.*, 1992, **1**, 179.
77 J. Jonkers, M. Bakker and J. A. M. van der Mullen, *J. Phys. D*, 1997, **30**, 1928.
78 J. Jonkers, PhD Thesis, Eindhoven Technical University, 1998.
79 H. G. Slottow, *IEEE Trans. Electron. Devices*, 1976, **23**, 760.
80 *Flat Panel Displays and CRT's*, ed. L. E. Tannas, Jr., Van Rostrand Reinhold, New York, 1985.

81 A. Sobel, *IEEE Trans. Plasma Sci.*, 1991, **19**, 1032.
82 K. Takahashi, *Display Devices*, 1996, **13**, 31.
83 S. V. Berezhnoi, I. D. Kaganovich, L. D. Tsendin and V. A. Schweigert, *Appl. Phys. Lett.*, 1996, **69**, 2341.
84 Y. T. Lee, M. A. Lieberman, A. J. Lichtenberg, F. Bose, H. Baltes and R. Patrick, *J. Vac. Sci. Technol. A*, 1997, **15**, 113.
85 J.-P. Boeuf, *Phys. Rev. A*, 1987, **36**, 2782.
86 J. D. P. Passchier and W. J. Goedheer, *J. Appl. Phys.*, 1993, **73**, 1073.
87 I. Abril, *Comput. Phys. Commun.*, 1988, **51**, 413.
88 R. J. Carman, *J. Phys. D.*, 1989, **22**, 55.
89 M. J. Kushner, *IEEE Trans. Plasma Sci.,* 1986, **14**, 188.
90 Z. Donko, K. Rozsa and R. C. Tobin, *J. Phys. D*, 1996, **29**, 105.
91 M. Surendra and D. B. Graves, *IEEE Trans. Plasma Sci.*, 1991, **19**, 144.
92 H. B. Smith, C. Charles, R. W. Boswell and H. Kuwahara, *J. Appl. Phys.*, 1997, **82**, 561.
93 M. Surendra, D. B. Graves and G. M. Jellum, *Phys. Rev. A*, 1990, **41**, 1112.
94 F. Y. Huang and M. J. Kushner, *J. Appl. Phys.*, 1995, **78**, 5909.
95 Z. Donko, *Phys. Rev. E*, 1998, **57**, 7126.
96 J. Vlcek, *J. Phys. D*, 1989, **22**, 623.
97 B. van der Sijde, J. J. A. M. van der Mullen and D. C. Schram, *Beitr Plasmaphys.*, 1984, **5**, 447.
98 C. Punset, J. P. Boeuf and L. C. Pitchford, *J. Appl. Phys.*, 1998, **83**, 1884.
99 L. C. Pitchford, I. Peres, K. B. Liland, J. P. Boeuf and H. Gielen, *J. Appl. Phys.*, 1997, **82**, 112.
100 A. Bogaerts, M. van Straaten and R. Gijbels, *Spectrochim. Acta*, *Part B*, 1995, **50**, 179.
101 A. Bogaerts, R. Gijbels and W. J. Goedheer, *J. Appl. Phys.*, 1995, **78**, 2233.
102 A. Bogaerts and R. Gijbels, *Phys. Rev. A*, 1995, **52**, 3743.
103 A. Bogaerts and R. Gijbels, *J. Appl. Phys.*, 1996, **79**, 1279.
104 A. Bogaerts, R. Gijbels and W. J. Goedheer, *Anal. Chem.*, 1996, **68**, 2296.
105 A. Bogaerts and R. Gijbels, *Anal. Chem.*, 1996, **68**, 2676.
106 A. Fiala, L. C. Pitchford, J. P. Boeuf and S. Baude, *Spectrochim. Acta*, *Part B*, 1997, **52**, 531.
107 A. Bogaerts, R. Gijbels and J. Vlcek, *J. Appl. Phys.*, 1998, **84**, 121.
108 A. Bogaerts, R. Gijbels and R. J. Carman, *Spectrochim. Acta*, *Part B*, 1998, **53**, 1679.
109 A. Bogaerts and R. Gijbels, *Anal. Chem.*, 1997, **69**, 719A.
110 A. Bogaerts and R. Gijbels, *J. Anal. At. Spectrom.*, 1998, **13**, 945.
111 A. Bogaerts and R. Gijbels, *J. Anal. At. Spectrom.*, 1996, **11**, 841.
112 A. Bogaerts, R. Gijbels and J. Vlcek, *Spectrochim. Acta*, *Part B*, 1998, **53**, 1517.
113 A. Bogaerts and R. Gijbels, *J. Anal. At. Spectrom.*, 1998, **13**, 721.
114 A. Bogaerts and R. Gijbels, *Spectrochim. Acta*, *Part B*, 1997, **52**, 765.
115 A. Bogaerts and R. Gijbels, *J. Anal. At. Spectrom.*, 1997, **12**, 751.
116 A. Bogaerts and R. Gijbels, *J. Am. Soc. Mass Spectrom.*, 1997, **8**, 1021.
117 A. Bogaerts, E. Wagner, B. W. Smith, J. D. Winefordner, D. Pollmann, W. W. Harrison and R. Gijbels, *Spectrochim. Acta*, *Part B*, 1997, **52**, 205.
118 D. E. Gray, *American Institute of Physics Handbook*, McGraw-Hill, New York, 3rd edn., 1972.
119 C. Jonkers, PhD Thesis, University of Antwerp, 1995.
120 V. Hoffmann, H.-J. Uhlemann, F. Prässler, K. Wetzig and D. Birus, *Fresenius' J. Anal. Chem.*, 1996, **355**, 826.
121 A. Bogaerts, R. Gijbels and W. J. Goedheer, *Jpn. J. Appl. Phys.*, in the press.
122 A. Bogaerts and R. Gijbels, *IEEE Trans. Plasma Sci.*, in the press.

Paper 9/00772E